

Dalton Transactions

Accepted Manuscript



This is an *Accepted Manuscript*, which has been through the Royal Society of Chemistry peer review process and has been accepted for publication.

Accepted Manuscripts are published online shortly after acceptance, before technical editing, formatting and proof reading. Using this free service, authors can make their results available to the community, in citable form, before we publish the edited article. We will replace this *Accepted Manuscript* with the edited and formatted *Advance Article* as soon as it is available.

You can find more information about *Accepted Manuscripts* in the [Information for Authors](#).

Please note that technical editing may introduce minor changes to the text and/or graphics, which may alter content. The journal's standard [Terms & Conditions](#) and the [Ethical guidelines](#) still apply. In no event shall the Royal Society of Chemistry be held responsible for any errors or omissions in this *Accepted Manuscript* or any consequences arising from the use of any information it contains.



**A fluorescent, photochromic and thermochromic
trifunctional material based on a layered metal-viologen
complex**

Journal:	<i>Dalton Transactions</i>
Manuscript ID	DT-COM-09-2015-003405.R1
Article Type:	Communication
Date Submitted by the Author:	21-Sep-2015
Complete List of Authors:	Wan, Fang; Fuzhou University, Chemistry Qiu, Li-Xia; Fuzhou University, Chemistry Zhou, Liang; Fuzhou University, Chemistry Sun, Yan-Qiong; Fuzhou University, Chemistry You, Yi; Fuzhou University,

SCHOLARONE™
Manuscripts

Stability and Toxicity of *Tris*-tolyl Bismuth(V) Dicarboxylates and their Biological Activity towards
Leishmania major

Yih Ching Ong,^a Victoria L. Blair,^a Lukasz Kedzierski,^b Kellie L. Tuck,^a and Philip C. Andrews^{a*}

^aSchool of Chemistry, Monash University, Clayton, Melbourne, VIC 3800, Australia

^bWalter and Eliza Institute of Medical Research, Parkville, Melbourne, VIC 3052 and Department of Medical Biology, University of Melbourne, Parkville 3010, Australia

*Email: phil.andrews@monash.edu

Abstract

A series of 29 *tris*-tolyl bismuth(V) di-carboxylato complexes of composition $[\text{Bi}(\text{Tol})_3(\text{O}_2\text{CR})_2]$ involving either *ortho*, *meta* or *para* substituted tolyl ligands have been synthesized and characterised. Of these 15 were assessed for their toxicity towards *Leishmania* promastigotes and human fibroblast cells, with ten then being subsequently assessed against parasite amastigotes. The carboxylate ligands are drawn from a series of substituted and biologically relevant benzoic acids which allow a comparison with earlier studies on $[\text{BiPh}_3(\text{O}_2\text{CR})_2]$ and analogous Sb(V) $[\text{SbAr}_3(\text{O}_2\text{CR})_2]$ (Ar = Ph and Tol) complexes. Twelve complexes have been structurally characterized by single crystal X-ray diffraction and shown to adopt a typical trigonal bipyramidal geometry in which the three tolyl ligands occupy the equatorial plane. NMR studies on two illustrative examples indicate that the complexes are stable in D_2O and DMSO but only have a half-life of 1.2 hours in culture medium, with glucose being a contributing factor in decomposition and reduction to $\text{Bi}(\text{Tol})_3$. Despite their short lifetime many complexes show significant toxicity towards promastigotes at low concentration ($< 6 \mu\text{M}$) and at that concentration provide for good selectivity indices (parasite vs mammalian cells), for example 114 for $[\text{Bi}(o\text{-Tol})_3(\text{O}_2\text{CC}_6\text{H}_3(2\text{-OH},5\text{-C}_6\text{H}_3(2,4\text{-F}_2)))_2]$ and 838 for $[\text{Bi}(m\text{-Tol})_3(\text{O}_2\text{CC}_6\text{H}_4(2\text{-OAc}))_2]$. Best activity and selectivity is observed with complexes containing *o*- and *m*-tolyl ligands, and it appears the primary influence on fibroblast toxicity is the Ar ligand while the carboxylate influences promastigote toxicity. The complexes are less effective *in vitro* against the parasite amastigotes, where longer incubation times and harsher chemical and biological environments are encountered in the assay. Nevertheless, there were some statistically relevant differences at $1 \mu\text{M}$ against the positive controls with the best performing complexes being $[\text{Bi}(o\text{-Tol})_3(\text{O}_2\text{CC}_6\text{H}_4(2\text{-EtO}))_2]$ and $[\text{Bi}(m\text{-Tol})_3(\text{O}_2\text{CC}_6\text{H}_4(2\text{-OAc}))_2]$

Introduction

Leishmaniasis is a group of diseases caused by the *Leishmania* parasite and transmitted via infected female sandflies. Visceral leishmaniasis (VL), the most serious form of the disease, affects the internal organs and without treatment is normally fatal within two years.¹ The World Health Organisation estimates that 300,000 cases of VL have been reported in the past 5 years with over 20,000 deaths annually, and 310 million people are currently at risk of infection.²

For more than 70 years the frontline treatment for leishmaniasis has been pentavalent antimonials; sodium stibogluconate (Pentostam; SSG)³ and meglumine antimoniate (Glucantime),⁴ which are readily available and cost-effective. However, they have severe and toxic side effects, and due to their parenteral mode of administration over a 28-day period compliance can be low⁵ and areas of drug resistance have appeared, such as Bihar in India.^{6, 7} Alternative treatments such as liposomal Amphotericin B⁸ and Miltefosine⁹ are available, however their prohibitive cost makes access to the drug difficult for the majority of patients. Furthermore, liposomal Amphotericin B is still administered intravenously, and Miltefosine, the only orally available drug has a narrow therapeutic window and is teratogenic.⁹ These challenges mean that there is a need for alternative, low cost, safe oral treatments with reduced toxicity and side effects.

Pentavalent antimony itself is relatively non-toxic and serves as a pro-drug which is reduced by trypanothione, glutathione or thiol-dependent reductase, TDR1 at pH 5 to the active Sb(III) species within the macrophage.^{10, 11} This leads to a decrease in buffering ability and imbalance in thiol redox potential as Sb(III) induces the efflux of trypanothione and glutathione out of the cell and their respective disulfides accumulate inside cells.¹² It is suggested that the redistribution of the Sb(III) species out of the parasite is responsible for the toxic effects.¹⁰

In seeking more lipophilic alternatives to SSG we have shown that several organometallic Sb(V) dicarboxylato complexes of general form $[\text{SbAr}_3(\text{O}_2\text{CR})_2]$ are promising leads, being highly effective against both promastigotes and amastigotes at very low concentrations (0.5-3.5 μM) while maintaining low toxicity towards human fibroblasts.¹³ Considering the periodic relationship of antimony and bismuth, and the low systemic toxicity of bismuth in humans,¹⁴ we extended our explorations to both Bi(III)^{15, 16, 17} and Bi(V)¹⁸ based compounds as promising candidates for future anti-leishmanial drugs, targeting decreased toxicity, reduced side effects, and greater potential for oral delivery. To that end we recently reported the chemistry and biological activity of a series of $[\text{BiPh}_3(\text{O}_2\text{CR})_2]$ complexes towards *L. major* promastigotes and human fibroblasts,¹⁸ showing that while $[\text{BiPh}_3(\text{O}_2\text{CR})_2]$ complexes show good activity against promastigotes, they were much less stable than their Sb(V) analogues,¹³ and were also non-selectively toxic against the fibroblasts, even at low concentrations. Using one complex, $[\text{BiPh}_3(\text{O}_2\text{CC}_6\text{H}_3(m\text{-OH})_2)_2]$ as an illustrative example, we showed the complexes to be stable in water and DMSO but to be unstable in culture medium,

undergoing oxidative decomposition to reform and precipitate BiPh_3 .¹⁸ However, the decomposition process was slow enough that the complex was still able to exert substantial toxic effects.

In our extensive study on $[\text{SbAr}_3(\text{O}_2\text{CR})_2]$ complexes we found that it was not those derived from SbPh_3 which proved to be the most promising, but complexes in which $\text{Ar} = m\text{-}$ or $p\text{-tolyl}$.¹³ Therefore, to establish a much closer comparison we undertook an assessment of the tolyl based complexes and here report on the synthesis and characterization of 29 organometallic *tris*-tolylbismuth(V) dicarboxylate complexes $[\text{Bi}(\text{Tol})_3(\text{O}_2\text{CR})_2]$ (where $\text{Ar} = o\text{-}, m\text{-}, p\text{-Tol}$) and their subsequent solubility and biological activity against *Leishmania major* promastigotes and human fibroblast cells. The most promising complexes were subsequently assessed on *L. major* amastigotes. Ten complexes and two starting compounds, shown in Figure 1 below, were found to have good anti-leishmanial activity with low fibroblast toxicity.

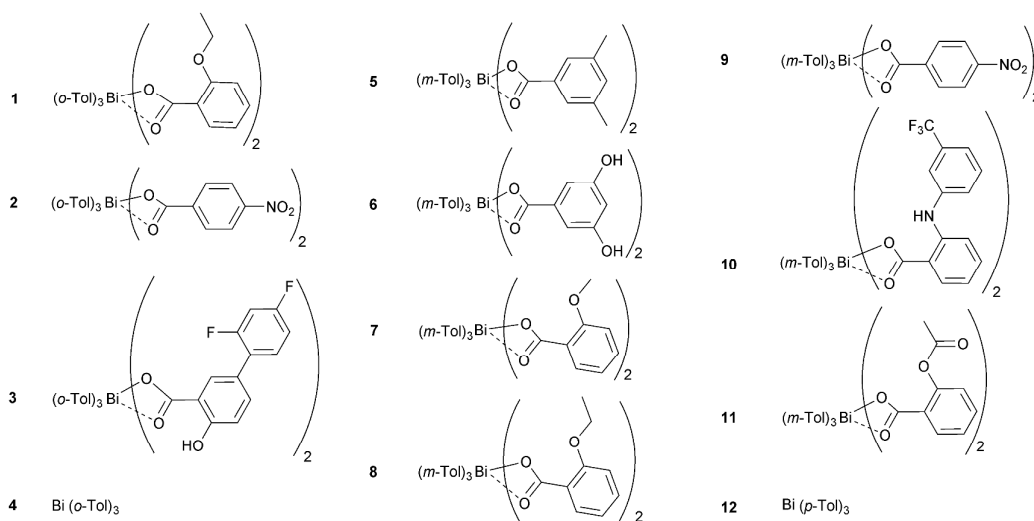
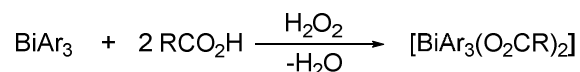


Figure 1. *Tris*-tolylbismuth(V) dicarboxylate complexes **1-3**, **5-11** and $\text{Bi}(\text{Tol})_3$, **4** and **12** studied for anti-leishmanial activity on promastigotes and amastigotes.

Results and discussion

The target $[\text{Bi}(\text{Tol})_3(\text{O}_2\text{CR})_2]$ (*o*-, *p*- or *m*-Tolyl) complexes were formed through an oxidative addition reaction between $\text{Bi}(\text{Tol})_3$ and the chosen benzoic acid promoted by hydrogen peroxide in a 1 : 2 : 1 stoichiometric ratio in diethyl ether at room temperature.¹⁹ After 30 minutes each reaction mixture was filtered and the resulting colourless solutions allowed to stand overnight. This resulted in the isolation of a suite of $[\text{Bi}(\text{Tol})_3(\text{O}_2\text{CR})_2]$ complexes as microcrystalline solids.



Scheme 1. General synthesis of *tris*-aryl bismuth(V) dicarboxylate complexes

The composition of the final products as $[\text{Bi}(\text{Tol})_3(\text{O}_2\text{CR})_2]$ was confirmed through ^1H and ^{13}C NMR spectroscopy, melting point, FT-IR spectrometry, mass spectrometry and elemental analysis. In addition, the diflunisal (difH) derived complex, $[\text{Bi}(o\text{-Tol})_3(\text{dif})_2]$, **3**, was analysed by single crystal X-ray diffraction. Full analytical details for **1-3** and **5-11** are given in the Experimental section while for all other complexes are provided in the Supplementary Information.

Table 1. Synthesis of $[\text{Bi}(\text{Tol})_3(\text{O}_2\text{CR})_2]$ complexes **1-3**, **5-11** with their melting points and yields

Complex	Carboxylic acid (code)	Ar	R	mp (°C)	Yield (%)
1	2-ethoxybenzoic acid	<i>o</i> -Tol	2-EtOC ₆ H ₄	126-128	39.0
2	4-nitrobenzoic acid	<i>o</i> -Tol	4-NO ₂ C ₆ H ₄	146-148	44.6
3	Diflunisal (difH)	<i>o</i> -Tol	2-OH,5-C ₆ H ₃ (2,4-F ₂)C ₆ H ₃	153-154	75.1
5	3,5-dimethylbenzoic acid	<i>m</i> -Tol	3,5-Me ₂ C ₆ H ₃	173-176	51.5
6	3,5-dihydroxybenzoic acid	<i>m</i> -Tol	3,5-(OH) ₂ C ₆ H ₃	170 (dec.)	64.6
7	2-methoxybenzoic acid	<i>m</i> -Tol	2-MeOC ₆ H ₄	145-146	47.6
8	2-ethoxybenzoic acid	<i>m</i> -Tol	2-EtOC ₆ H ₄	144-145	46.2
9	4-nitrobenzoic acid	<i>m</i> -Tol	4-NO ₂ C ₆ H ₄	170-172	41.9
10	Flufenamic acid	<i>m</i> -Tol	2-NH(C ₆ H ₄ -3-CF ₃)C ₆ H ₄	143-147	66.4
11	Aspirin (aspH)	<i>m</i> -Tol	2-OAcC ₆ H ₄	129-132	76.9

Depending on the solubilities of the final products, NMR spectra were collected in either CDCl₃ or D₆-DMSO at room temperature. The chemical shifts and integrals all corresponded with formation of the target $[\text{Bi}(\text{Tol})_3(\text{O}_2\text{CR})_2]$ complexes. All complexes showed low frequency shifts in the *ortho*, *meta* and *para* proton resonances of the tolyl ligand compared to the corresponding protons in Bi(Tol)₃. The –OH signal corresponding to the –COOH of the carboxylic acid, observed in the ^1H NMR spectra of the parent acids between 11.61 – 13.67 ppm, was also absent indicating deprotonation and complexation of the carboxylates to the Bi atom.

Compared to the parent acids which have their carboxylic acid carbonyl stretches in the range of 1650-1700 cm⁻¹, all the complexes show a shift to a lower wavenumber for their carboxylate carbonyl asymmetric and symmetric stretches to 1540-1650 cm⁻¹ and 1300-1420 cm⁻¹. This indicates the deprotonation of the –COOH functionality to form the $[\text{Bi}(\text{Tol})_3(\text{O}_2\text{CR})_2]$ complex. The difference between the symmetric and asymmetric shifts are less than 200 cm⁻¹ for all the complexes. According to Deacon and Philips,²⁰ this indicates that the carboxylate ligands adopt a bidentate chelating mode to the bismuth centre, and this trend was observed also in the solid state structures of the $[\text{BiPh}_3(\text{O}_2\text{CR})_2]$ complexes.¹⁸

X-Ray Crystallography

Of the 29 complexes synthesised crystals suitable for single crystal X-ray diffraction studies were obtained for 11 of them: $[\text{Bi}(o\text{-Tol})_3(\text{dif})_2]$ **3**, $[\text{Bi}(m\text{-Tol})_3(\text{O}_2\text{CC}_6\text{H}_3(2,5\text{-OH}))_2]$ **6**, $[\text{Bi}(m\text{-Tol})_3(\text{O}_2\text{CC}_6\text{H}_4(2\text{-EtO}))_2]$ **8**, $[\text{Bi}(m\text{-Tol})_3(\text{O}_2\text{CC}_6\text{H}_4(4\text{-NO}_2))_2]$ **9**, $[\text{Bi}(m\text{-Tol})_3(\text{O}_2\text{CC}_6\text{H}_3(2\text{-OH},5\text{-Cl}))_2]$ **19**, $[\text{Bi}(m\text{-Tol})_3(\text{O}_2\text{CC}_6\text{H}_4(2\text{-NHC}_6\text{H}_3(2\text{-Me},3\text{-Cl}))_2)]$ **22**, $[\text{Bi}(p\text{-Tol})_3(\text{O}_2\text{CC}_6\text{H}_4(2\text{-OMe}))_2]$ **25**, $[\text{Bi}(p\text{-Tol})_3(\text{O}_2\text{CC}_6\text{H}_4(2\text{-OEt}))_2]$ **26**, $[\text{Bi}(p\text{-Tol})_3(\text{O}_2\text{CC}_6\text{H}_4(4\text{-NO}_2))_2]$ **27**, $[\text{Bi}(p\text{-Tol})_3(\text{O}_2\text{CC}_6\text{H}_3(2\text{-OH},5\text{-Cl}))_2]$ **28** and $[\text{Bi}(p\text{-Tol})_3(\text{O}_2\text{CC}_6\text{H}_4(2\text{-NHC}_6\text{H}_3(2\text{-Me},3\text{-Cl}))_2)]$ **31**. The complexes are isostructural and discussion on **3** is provided here as an illustrative example. Figures depicting the solid-state structures of the other complexes along with a summary of their bond lengths and crystallographic data are provided as Electronic Supporting Information.

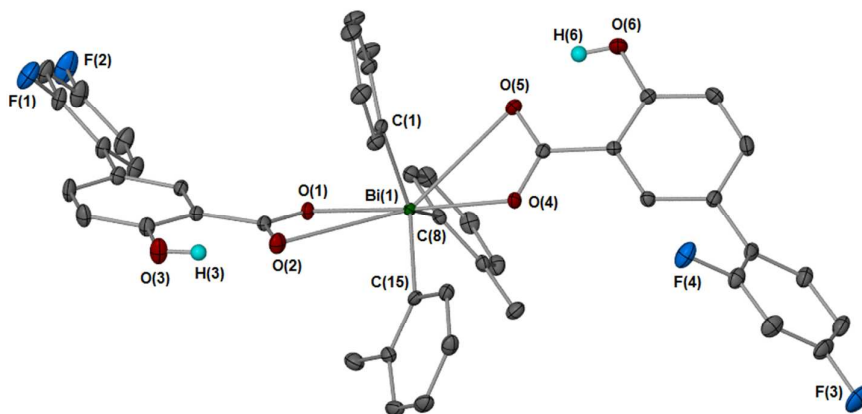


Figure 2. Molecular structure of $[\text{Bi}(o\text{-Tol})_3(\text{dif})_2]$, **3** showing thermal ellipsoids at 50% probability. Hydrogen atoms have been omitted for clarity. Selected bond lengths(Å) and bond angles(°): Bi(1)-C(15) 2.208(2); Bi(1)-C(1) 2.216(2); Bi(1)-C(8) 2.223(2); Bi(1)-O(4) 2.2764(15); Bi(1)-O(1) 2.2936(15); Bi(1)-O(5) 3.0740(16); Bi(1)-O(2) 3.0813(17); C(15)-Bi(1)-C(1) 110.62(8); C(15)-Bi(1)-C(8) 116.29(8); C(1)-Bi(1)-C(8) 132.94(8); O(4)-Bi(1)-O(5) 46.22(5); O(1)-Bi(1)-O(2) 46.02(5).

Suitable single crystals of $[\text{Bi}(o\text{-Tol})_3(\text{dif})_2]$, **3** were obtained from a THF/*n*-hexane mixture through slow evaporation. As shown in Figure 2 the complex adopts a typical distorted trigonal bipyramidal geometry. The tolyl ligands sit in the equatorial plane with a propeller-like orientation, while the carboxylates sit in the axial positions. All the Bi-C bond lengths are similar; Bi(1)-C(15) 2.208(2), Bi(1)-C(1) 2.216(2), Bi(1)-C(8) 2.223(2). However, one of the C-Bi-C trigonal angles is more obtuse than the rest (*cf.* 132.94(8) vs 110.62(8) and 116.29(8)), leading to a distortion towards square pyramidal based geometry. The oxygen atoms of the carboxylate moieties are bound to the bismuth centre in a bidentate fashion confirming observation in the IR spectrum. The second carboxyl (C=O) oxygen atoms, O(2) and O(5) of the carboxylate ligands, have longer Bi-O distances, 3.0740(16) Å and 3.0813(17) Å, as compared to the two shorter Bi-O bonds 2.2764(15) Å and 2.2936(15) Å. For this complex, the presence of an *ortho*-OH functionality on the phenyl ring of the carboxylate ligand forms a hydrogen bond to the oxygen of the carboxylate, and may contribute to the longer Bi-O bond length.

This structure for the $[\text{Bi}(\text{Tol})_3(\text{O}_2\text{CR})_2]$ analogues are similar to that observed for the $[\text{BiPh}_3(\text{O}_2\text{CR})_2]$ complexes.¹⁸ For example, the analogous $[\text{BiPh}_3(\text{dif})_2]$ complex also shows a distorted trigonal bi-pyramidal structure. A comparison between the phenyl and tolyl analogues shows that the bond lengths; Bi-C (2.204(8) Å, 2.217(12) Å) and Bi-O (2.253(6) Å, 3.041(7) Å), are similar and are only slightly shorter than those in $[\text{Bi}(\text{Tol})_3(\text{dif})_2]$; Bi-C (2.208(3), 2.2218(3), 2.227(3) Å) and Bi-O (2.227(2), 2.293(2), 3.073(2), 2.081(2) Å). This indicates that the presence of an additional *o*-Me group on the phenyl ring has little influence on the structure of the complex. Conversely, the analogous Sb-C bonds in the Sb(V) complex $[\text{SbPh}_3(\text{O}_2\text{CCH}_2\text{C}_6\text{H}_4(m\text{-CH}_3))_2]$ are 2.0949(14), 2.0974(14) and 2.1105(13) Å, and the Sb-O bonds are 2.0880(9) Å and 2.1108(10) Å, with the carboxylate ligands binding in a monodentate manner.

Stability studies

To determine whether the complexes are stable to atmospheric moisture and gases, all complexes were exposed to air and screened by melting point over a period of six months. There was no change in the observed melting points over this time, indicating the complexes have a high degree of stability in the solid-state. Short-term stability in solution was evaluated through the ¹H NMR spectrum of each complex being collected and compared at *t* = 0 and 48 h in either CDCl₃ or D₆-DMSO. No change in the chemical shifts was observed.

In our earlier studies on $[\text{BiPh}_3(\text{O}_2\text{CR})_2]$ complexes we used $[\text{BiPh}_3(\text{O}_2\text{CC}_6\text{H}_3(2,5\text{-OH}))_2]$ as an example to study and understand the stability of the complex in culture medium.¹⁸ While the complex was found to be stable in water and DMSO, decomposition was found to occur in DMEM culture media to precipitate the starting reagent BiPh₃ as a white precipitate. A subsequent NMR study showed that the complex was stable to phosphate (or other anion) exchange and did not react with the amino acids in solution, noting that the key amino acid primed for oxidation, cysteine, is already present in DMEM in its oxidised state.¹⁸

Similar studies were therefore conducted on $[\text{Bi}(o\text{-Tol})_3(\text{dif})_2]$, **3** as a representative example of the Bi(V)-tolyl series of complexes. To assess stability in cell culture medium, ¹H NMR spectral data was collected at *t* = 0 h and 48 h. Conditions similar to those used in the biological assay were used, however the signal-to-noise ratio for the highest concentration used in the *in vitro* biological assay (100 μM) was too low to provide any meaningful data and, as such, a sample concentration of 1.0 mM was used. The culture medium was freeze-dried and reconstituted in D₂O to minimise the H₂O signal. Complex **3** was added to the culture medium and the resulting mixture allowed to stand for 24 hours, resulting in the formation of a white precipitate. The supernatant was then decanted off, and the white precipitate dissolved in d₆-DMSO and analysed by ¹H NMR. By comparing the chemical shifts produced by the unknown white precipitate, it was deduced that the precipitate was the starting reagent Bi(*o*-Tol)₃. (Figure 4) This was confirmed by a

comparison of the melting point which showed the unknown white precipitate (mp. 130 °C) was consistent with $\text{Bi}(o\text{-Tol})_3$ (mp. 132 °C), as opposed to **3** (mp. 154 °C). This indicated that over time the Bi(V) complex **3** was being reduced.

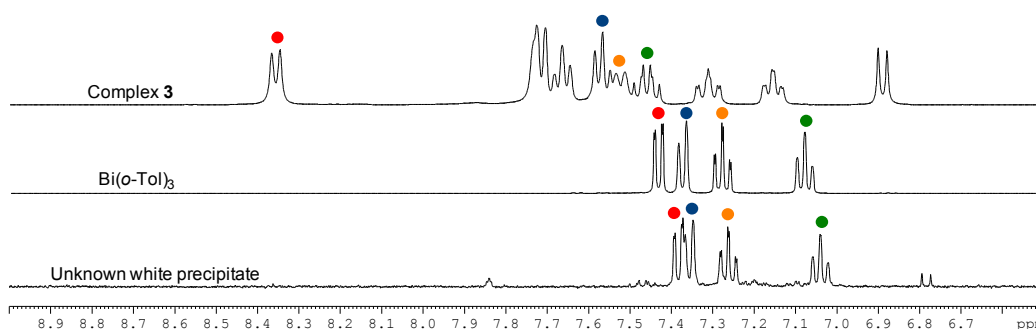


Figure 4. ^1H NMR spectra comparison of unknown white precipitate with $[\text{Bi}(o\text{-Tol})_3(\text{dif})_2]$, **3** & $\text{Bi}(o\text{-Tol})_3$ in the aromatic region. Coloured dots indicate the chemical shifts for the respective tolyl protons.

To determine the rate of decomposition, a ^1H NMR spectrum of **3** in culture medium was recorded every 30 mins for 10 hours. Using the integration of one chemical shift from the culture medium at 4.4 ppm as a standard, the decrease in integration of the *ortho* proton in **3** was measured. It was found that the integration fell from 1.000 ($t = 0$ h) to 0.0245 after 4.5 hours and then to 0.000 after 5 hours. The plot, shown in Figure 5, followed a one-phase exponential decay ($R^2 = 0.9955$) with a half-life of 1.2 hours. This indicated that even though the complexes have a short half-life, they have potent anti-parasitic activity while being non-toxic towards human fibroblast cells.

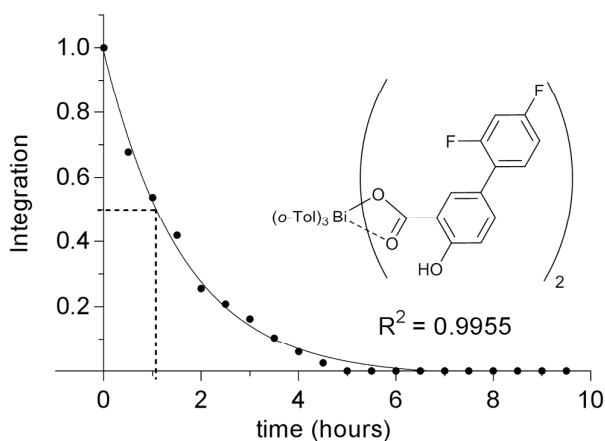


Figure 5. Decomposition curve of $[\text{Bi}(o\text{-Tol})_3(\text{dif})_2]$, **3** in DMEM culture media at 25 °C with time.

It is still not clear what is oxidised as the Bi(V) complex reduces to BiAr_3 . One of the principle constituents of culture medium (DMEM and M199) is glucose, second only to NaCl in concentration. Initial NMR spectra

looking at the interaction of **3** with glucose proved complicated, so to simplify the data the aspirin (aspH) derivative $[\text{Bi}(m\text{-Tol})_3(\text{asp})_2]$, **11** was chosen as the illustrative Bi(V) complex for the study.

Glucose was added to $[\text{Bi}(m\text{-Tol})_3(\text{asp})_2]$ **11** in d_6 -DMSO in a stoichiometric ratio of 2:1, and the ^1H NMR spectrum recorded at $t = 0$, 48 h, and 1 week, at room temperature (20 °C). Control studies showed that when the individual species were left to stand in d_6 -DMSO, there were no changes in the spectrum. However, when both **11** and glucose were added together, after 48 h significant changes in the chemical shifts of **11** and glucose were observed (Figure 6). Integrations of the initial signals of **11** and glucose decreased, while signals matching that of starting reagent $\text{Bi}(m\text{-Tol})_3$ appeared. In the range of the aromatic region at $t = 48$ h, both complex **11** and $\text{Bi}(m\text{-Tol})_3$ are present in solution. However after 1 week, only the $\text{Bi}(m\text{-Tol})_3$ could be observed.

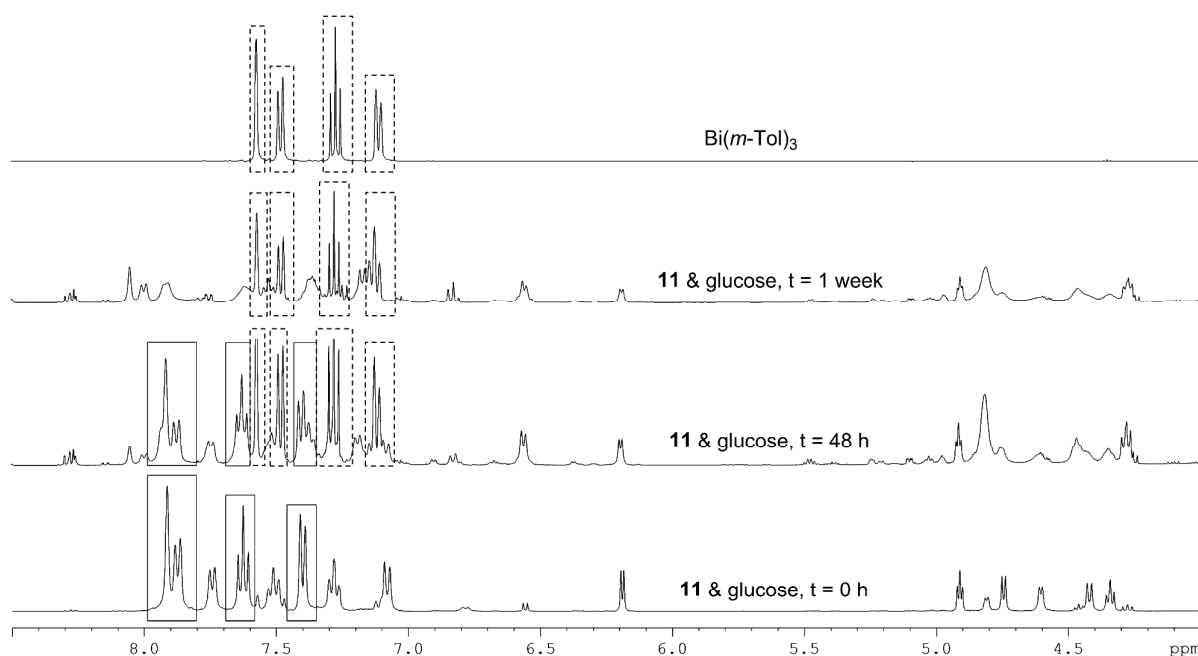


Figure 6. ^1H NMR spectroscopic studies of $[\text{Bi}(m\text{-Tol})_3(\text{asp})_2]$ **11** and glucose in d_6 -DMSO, 25 °C at $t = 0$ h, $t = 48$ h, and $t = 1$ week. Dotted boxes are drawn around the chemical signals of $\text{Bi}(m\text{-Tol})_3$ and solid boxes are drawn around the corresponding tolyl chemical signals of **11**.

This experiment was repeated, this time with **11** and glucose stirred at 40 °C over 18 hours. The resulting ^1H NMR spectrum resembled that of $t = 48$ h at 25 °C, where both **11** and $\text{Bi}(m\text{-Tol})_3$ were present, indicating that the rate of decomposition of **11** increases at higher temperatures. However, the rate of decomposition is not comparable with that observed in the culture medium (5 h in culture medium vs 1 week in DMSO), suggesting that while glucose is a component of the decomposition process, other, as yet unknown, factors contribute to an accelerated rate of decay.

Biological Activity

L. major promastigotes and human fibroblast cells

All complexes were first screened for solubility in DMSO (see ESI). A total of fifteen Bi(V) complexes **1-3**, **5-11**, **25-29**, their parent benzoic acids along with Bi(*o*-Tol)₃, **4**, Bi(*m*-Tol)₃, **36** and Bi(*p*-Tol)₃, **12** were assessed for their anti-parasitic activity on *L. major* promastigotes and their toxicity towards human fibroblast cells. Insoluble complexes were excluded from the assay. The complexes were tested over concentration range of 48 nM to 100 μM in culture media from a 10 mM DMSO stock. The resulting IC₅₀ values are presented in Table 2. DMSO and Amphotericin B controls were set up at concentrations equivalent to that of the compound concentrations (48 nM to 100 μM). DMSO showed no apparent effect on any of the promastigotes or human fibroblast cells. Amphotericin B was the reference anti-leishmanial reagent. Complexes with a suitable selectivity index (parasites vs human cells) were taken forward into a study on their effectiveness towards amastigotes.

Table 2. IC₅₀ and selectivity ratios of Bi(Tol)₃ **4**, **36**, **12** and their derived complexes **1-3**, **5-11**, **25-29** respectively with *L. major* promastigotes and human fibroblasts

Complex [Bi(Tol) ₃ L ₂]	Ar	L	IC ₅₀ (± SEM) (μM)		Selectivity ratio: ($\frac{IC_{50} \text{ fibroblast}}{IC_{50} \text{ promastigotes}}$)	Selectivity index at 6.12 μM
			Promastigotes	Fibroblasts		
1	<i>o</i> -Tol	O ₂ CC ₆ H ₄ (2-EtO)	0.93 (0.04)	17.13 (0.05)	18.4	11.3
		O ₂ C C ₆ H ₄ (4-NO ₂)	0.69 (0.03)	14.21 (0.03)	20.6	42.4
		O ₂ CC ₆ H ₃ (2-OH,5-C ₆ H ₃ (2,4-F ₂))	0.57 (0.02)	16.13 (0.04)	28.3	114.1
		-	0.85 (0.03)	11.02 (0.03)	13.0	1.2
5	<i>m</i> -Tol	O ₂ CC ₆ H ₃ (3,5-Me ₂)	1.10 (0.04)	9.86 (0.02)	9.0	10.8
		O ₂ CC ₆ H ₃ (3,5-(OH) ₂)	1.11 (0.11)	11.19 (0.02)	10.0	2.0
		O ₂ CC ₆ H ₄ (2-MeO)	0.93 (0.04)	12.02 (0.01)	12.9	20.7
		O ₂ CC ₆ H ₄ (2-EtO)	0.89 (0.03)	11.52 (0.02)	12.9	21.0
		O ₂ CC ₆ H ₄ (4-NO ₂)	0.75 (0.05)	13.77 (0.02)	18.4	39.9
		O ₂ CC ₆ H ₄ (2-NH(C ₆ H ₄ (3-CF ₃)))	0.76 (0.02)	19.81 (0.04)	26.1	60.0
		O ₂ CC ₆ H ₄ (2-OAc)	0.76 (0.02)	11.96 (0.01)	15.7	838.0
		-	20.99 (0.05)	460.20 (0.29)	21.9	1.27
12	<i>p</i> -Tol	-	0.98 (0.02)	28.38 (0.04)	29.0	2.1
		O ₂ CC ₆ H ₃ (3,5-Me ₂)	0.84 (0.02)	5.55 (0.04)	6.6	6.0
		O ₂ CC ₆ H ₃ (3,5-(OH) ₂)	1.04 (0.02)	5.76 (0.05)	5.5	3.5
		O ₂ CC ₆ H ₄ (2-MeO)	1.04 (0.02)	5.82 (0.05)	5.6	4.6
		O ₂ CC ₆ H ₄ (2-EtO)	1.77 (0.02)	7.82 (0.03)	4.4	3.8
		O ₂ CC ₆ H ₄ (4-NO ₂)	0.89 (0.02)	4.48 (0.04)	5.0	3.7
		-	-	-	-	-

After 48 hours, the parent carboxylic acids showed no toxicity towards the parasites or the fibroblasts. In contrast, all of the bismuth complexes showed anti-promastigote activity. Ideally, Bi(V) complexes would show excellent bioactivity towards the promastigotes (low percentage viabilities) while maintaining non-toxicity towards human fibroblasts (high percentage viability). This would be an indication that the complex would be less toxic and so would have decreased harmful side effects. Most of the complexes tested also showed toxicity to human fibroblasts at concentrations above 12.5 μM . However, at lower concentrations, below 10 μM , compounds **1-12** showed distinct discrimination between the promastigotes and fibroblasts. Some compounds in this group performed well at one concentration, higher and lower concentrations tended not to give as desirable fibroblast/promastigote viabilities. Other compounds were able to perform well over a larger range of concentrations.

Compounds **2, 3, 9, 10** and **11** belong to this latter category. At 6.12 μM , promastigote viability ranged from 0.0 – 6.3 % and fibroblast viability of 83.8 - 100 %. At a complex concentration of 3.12 μM , promastigote viability was slightly higher, ranging from 0.4 – 21.9 %, with 100 % fibroblast viability.

Compounds **1, 5, 7** and **8** on the other hand belong to the first category. They had promastigote viabilities and fibroblast viabilities of 3.9 – 9 % and 82 – 100 % at 6.12 μM respectively, and 11.9 – 24 % and 92.7 – 100 % at 3.12 μM respectively. At a lower concentration of 3.12 μM , the lowest threshold reached by the complex in eradicating promastigotes was 11.9 %, while still maintaining a respectable >92 % viability for the fibroblasts. In comparison, the lower viability for the promastigotes at 6.12 μM also indicated that the fibroblasts were affected by the complex, giving the lowest fibroblast viability to be 82 %. In this case, compound **1** sustained a constant 100 % fibroblast viability while killing up to 91 % of the promastigotes at 6.12 μM , and 76 % promastigotes at 3.12 μM .

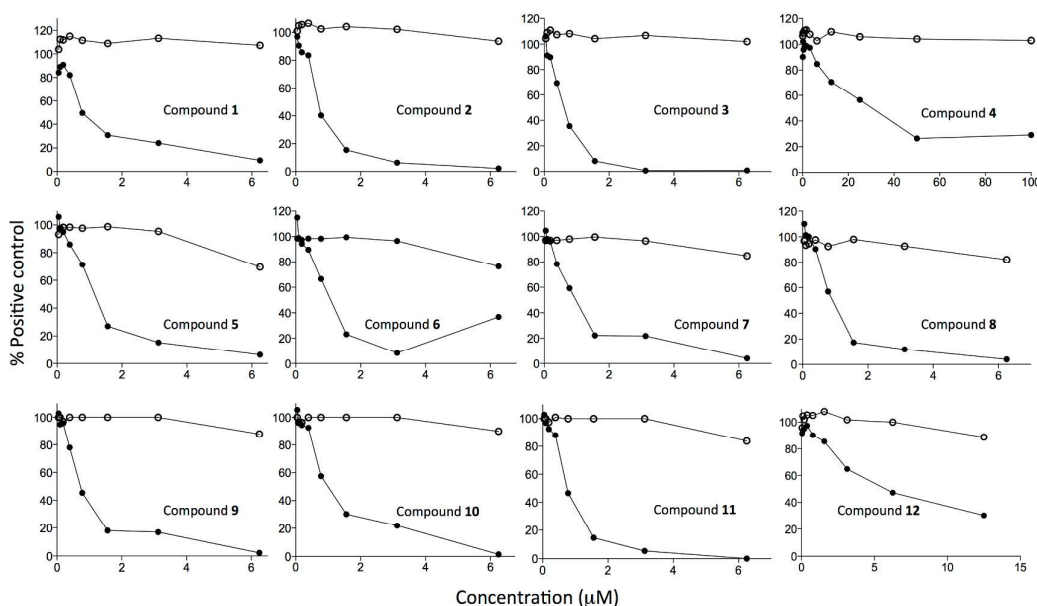


Figure 7. Activity of **1-12** on *L. major* promastigotes (●) and human fibroblasts (○) after 48 hours.

Selectivity

Our previous studies focused on two areas: the Sb(V) compounds derived from carboxylates of both non-NSAID and NSAID classes,¹³ and the Bi(III) compounds which were derived from NSAID and non-NSAID classes.¹⁵ With the Sb(V) compounds, it was determined that there was a trend in which *p*-Tol and *m*-Tol analogues were more promising than the *o*-Tol and Ph analogues by being more bioactive against both *L. major* promastigotes and amastigotes.¹³ With the Bi(V) compounds however, the trend was found to differ from that of the Sb(V) complexes.

Complexes derived from 4-nitrobenzoic acid were available for comparison across the entire tolyl series while compounds derived from 2-ethoxybenzoic acid were available for comparison across the aryl series of *o*-, *m*-, *p*-Tol and Ph.

Based on duplicate tests on fibroblasts and promastigotes, it became apparent that the primary influence on the non-toxicity of the complex was based on the aryl group while the activity against the promastigote was based on the carboxylate ligand. By looking at their IC₅₀ values, the general trend of selectivity observed across the series was identified as *o*-Tol ≥ *m*-Tol > *p*-Tol ≥ Ph.

For the promastigotes, [Bi(*o*-Tol)₃(O₂CC₆H₄(4-NO₂))₂] had the lowest IC₅₀ (0.69 ± 0.03 μM), followed closely by [Bi(*m*-Tol)₃(O₂CC₆H₄(4-NO₂))₂] (0.75 ± 0.04 μM), and then [Bi(*p*-Tol)₃(O₂CC₆H₄(4-NO₂))₂] (0.89 ± 0.02 μM). For the fibroblasts, the same trend was followed, with the *ortho* analogue having the highest IC₅₀ (14.21 ± 0.03 μM), followed very closely by *meta* (14.04 ± 0.02 μM) and *para* (4.48 ± 0.04 μM). This trend was also followed by compounds derived from 2-ethoxybenzoic acid, [Bi(Tol)₃(O₂CC₆H₄(2-EtO))₂].

For promastigotes, [Bi(*o*-Tol)₃(O₂CC₆H₄(2-EtO))₂] and [Bi(*m*-Tol)₃(O₂CC₆H₄(2-EtO))₂] had similar IC₅₀ values; (0.93 ± 0.04 μM) and (0.89 ± 0.03 μM) respectively, followed by [Bi(*p*-Tol)₃(O₂CC₆H₄(2-EtO))₂] at (1.77 ± 0.02 μM), and lastly [BiPh₃(O₂CC₆H₄(2-EtO))₂] at (2.29 ± 0.04 μM).¹⁸

For fibroblasts, a similar trend was followed as for the first set: the IC₅₀ values are highest for the *ortho* analogues (17.13 ± 0.05 μM), followed by the *meta* (11.63 ± 0.02 μM), *para* (0.89 ± 0.02 μM) and finally phenyl (3.84 ± 0.03 μM).¹⁸

From this comparison of IC₅₀ values across different aryl groups, it can be seen that the *ortho* and *meta* analogues were more selective and promising, while the *p*-Tol and the Ph series were relatively similar in terms of activity on both parasites and fibroblasts, and were not as selective. These complexes were therefore not included for future testing.

From the individual percentage viabilities at certain complex concentrations, we analysed the data to obtain the IC₅₀ for each complex based on their activity against promastigotes and fibroblasts. A selectivity index was calculated from the ratio of IC₅₀ of the fibroblasts to the IC₅₀ of the promastigotes. Compounds with a score ≥ 9.0 proceeded to further biological testing against *L. major* amastigotes. This excluded [Bi(*m*-Tol)₃] **36** and the [Bi(*p*-Tol)₃L₂] complexes **25-29**.

***L. major* amastigotes**

Based on their selectivity index, compounds **1-12** were assessed for their activity against *L. major* amastigotes, the clinically relevant form of the parasite. Amastigote-infected macrophages were incubated for 48 hours in the presence 1 μM complex concentration, selected based on IC_{50} values obtained from the promastigote assay.

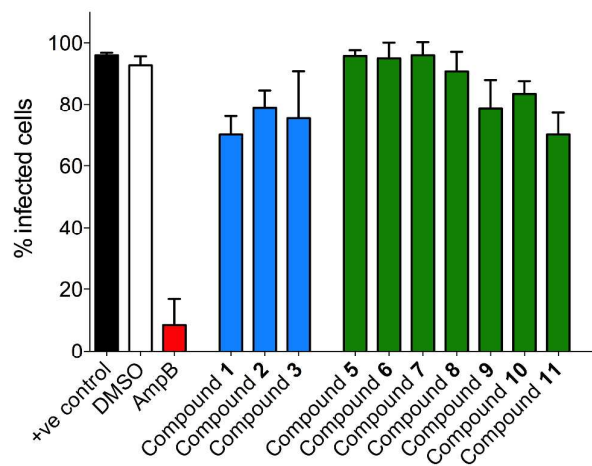


Figure 8. Infected macrophages after 48 hours. Number of macrophages infected with at least one amastigote was determined by microscopy of fixed specimens in duplicates. Amphotericin B (AmpB) was used as a reference compound at $0.5 \mu\text{g mL}^{-1}$. DMSO control was at 1 %. Error bars indicate SEM, one-way ANOVA with Dunnett's multiple comparison test was used to determine statistical significance between test samples and non-treated control (+ve control).

The macrophage invasion assay presents a more challenging biological environment and demands more from the complexes than the promastigote assay. Compounds have to traverse two membranes and be active in the acidic environment of phagolysosomes. Compounds **1, 2, 3, 9, and 11** showed anti-amastigote activity that resulted in statistically significant differences when compared to the positive control, while compounds **5, 6, 7, 8 and 10** displayed no anti-amastigote activity. Differences although significant, were small and do not appear physiologically relevant. Nevertheless, these data provide information regarding the structure-activity relationship. The more active and selective compounds were mostly the $[\text{Bi}(\textit{o}\text{-Tol})_3\text{L}_2]$ and $[\text{Bi}(\textit{m}\text{-Tol})_3\text{L}_2]$ complexes, though the *m*-Tol complexes displayed a greater range of toxicities based on their ligand combination. Compared to earlier assays performed with *tris*-arylantimony(V) dicarboxylates, the bismuth analogues were not as effective. Future complexes have to be designed to be more stable. The Bi(III) compounds $\text{Bi}(\textit{o}\text{-Tol})_3$ **4** and $\text{Bi}(\textit{p}\text{-Tol})_3$ **12**, products of the *in situ* reduction of the Bi(V) complexes were tested at a 10-fold higher concentration than the bismuth(V) complexes and showed some anti-parasitic activity.

It is not surprising to see low or no activity in the macrophage invasion assay. In the majority of cases promising results from promastigote testing cannot be extrapolated to amastigote setting.²¹ The short half-life of compounds could be responsible for relatively low levels of observed activity, particularly if they can only exert most of their toxicity towards the amastigotes during the first few hours in culture medium.

It is also possible that the concentration tested (the IC₅₀ value) was too low. Despite being sufficient to kill 50 % of promastigotes in culture that concentration was too low to be effective against amastigotes. It is reasonable to assume that this is due to a number of coincident factors: an inability of the compounds to cross macrophage membranes because of permeability constraints; inefficient uptake by parasites; rapid intracellular degradation; or inactivity in the more acidic environment. Moreover, non-optimized compounds were tested and it is unlikely that they would exhibit potent anti-leishmanial activities without further iterative rounds of medicinal chemistry optimisation. As such our ongoing efforts are aimed at structural modification to improve permeability and stability, and to focus on compounds encapsulation as a delivery system to the amastigotes.

Conclusion

A series of twenty-nine organometallic triarylbi-muth(V) dicarboxylates of the form [Bi(Tol)₃(O₂CR)₂] were synthesized and fully characterized. Eleven solid-state structures were determined by single crystal x-ray diffraction (**3**, **6**, **8**, **9**, **19**, **22**, **25-28**, **31**) showing the complexes adopt a typical trigonal bipyramidal geometry. The complexes are monomeric in the solid state with a seven coordinate Bi(V) centre. The carboxylate ligands adopt a bidentate binding mode to the Bi(V) atom, a general feature across the series of compounds as confirmed by FT-IR analysis.

Fifteen of the complexes were assessed for their anti-parasitic activity against *L. major* promastigotes and for cytotoxicity against human fibroblasts. All complexes were highly active against the promastigotes while the free acids proved to be non-toxic at the highest tested concentration of 100 μM. The primary influence on the non-toxicity of the complexes appears to be based mainly on the aryl group while the activity against the promastigote is based on the carboxylate ligand. IC₅₀ values showed the general trend of selectivity observed across the series to be *o*-Tol ≥ *m*-Tol > *p*-Tol ≥ Ph.

To assess the stability of the Bi(V) complexes, a representative example, complex [Bi(*o*-Tol)₃(dif)₂], **3** was studied in D₂O and DMSO and in DMEM cell culture medium. Resulting ¹H NMR spectra showed the complex to be stable in D₂O and DMSO, however in cell culture medium, [Bi(*o*-Tol)₃(dif)₂] was observed to reduce to its starting compound Bi(*o*-Tol)₃ which precipitates out as an off-white solid. Further solution state studies found the half-life of complex **3** to be 1.2 hours. While our previous studies have shown little impact of amino acids, phosphate or other anions on the decomposition of the Bi(V) complexes, ¹H NMR solution studies on the structurally simpler complex [Bi(*m*-Tol)₃(asp)₂], **11**, indicated that glucose, present in high concentration in DMEM and M199, does play a role in the decomposition though the rate is not as

fast as that observed when the complex is in culture medium meaning other, as yet unknown factors, contribute to the reduction of the Bi compounds.

Despite the rapid decomposition rate of the Bi(V) complexes in culture medium they are still active long enough to exert a significant, and somewhat selective, toxic effect on the promastigotes and fibroblasts. The decomposition products Bi(Tol)₃ are relatively non-toxic to both.

Based on their selectivity index, ten complexes derived mainly from Bi(*o*-Tol)₃ and Bi(*m*-Tol)₃ were further screened for amastigote and macrophage toxicity, representing the clinical form of the disease. In this assay the compounds did not perform as well reflecting the significantly more challenging biological environment, as well the inherent instability of the complexes under such conditions.

Acknowledgements

The authors thank the Australian Research Council, Monash University and the Walter and Eliza Institute of Medical Research for financial support, and Dr. Chris Tonkin (WEHI) for the supply of human primary fibroblast cells.

Experimental Section

All solvents used were purchased from Merck. For synthesis of BiPh₃, solvents were dried prior to use via the MBraun-SPS-800 and stored over molecular sieves (4Å) in a Schlenk flask under N₂. *Tris-o*-tolylbismuth, **4** and *tris-p*-tolylbismuth, **12** were synthesized via literature procedure.²² All other required chemicals were purchased from Sigma-Aldrich and used as received. NMR spectra were recorded on a Bruker Avance DRX400 spectrometer (400 MHz) with chemical shifts referenced to the appropriate deuterated solvents. Infrared spectra were recorded on an Agilent Technologies Cary 360 FTIR spectrometer in the range 4000-500 cm⁻¹. Melting points were determined in soda glass tubes on a digital Stuart Scientific melting point apparatus SMP10. Mass spectrometry (ESI) was performed on a Micromass Platform QMS spectrometer with an electrospray source and a cone voltage of 35 eV. CHN elemental analysis was performed by The Campbell Microanalytical Laboratory, Department of Chemistry, University of Otago in Dunedin, New Zealand.

Biological Assays

Cell viability assay: The Celltiter Blue Cell Viability Assay (Promega, Madison, WI, USA) was used for screening for anti-leishmanial activity and toxicity. Compounds were dissolved in DMSO at 10 mmol/L working stock and diluted out in appropriate culture media. The assay was set up in duplicates in 96-well plates according to the manufacturer's instructions. 10⁶ promastigotes/mL and 10⁵/mL primary human fibroblasts were used. Cell viability was assessed by measuring fluorescence at 550 nm excitation and 590 nm emission as per manufacturers' instructions.²³ The Celltiter Blue dye was added to samples at the time

of setting up the assay and the negative control (no cells) value was subtracted from all subsequent readings as a background value. The mean was calculated from duplicate readings. All readings were compared to the no-drug control and the percentage growth inhibition was calculated. DMSO controls were included. All plates were assessed microscopically. The graphs shown in this paper give the percentage of positive control versus concentration. Macrophage invasion assay was performed as previously described.²⁴

Cell culture: *Leishmania major* virulent clone V121 was derived from the *L. major* isolate LRC-L137 and maintained at 26 °C in M199 medium supplemented with 10% (v/v) heat inactivated FBS (Trace Biosciences, NSW, Australia).²⁵ The human primary fibroblast cells were cultured in Dulbecco's Modified Eagle's Medium (DMEM) (Life Technologies) supplemented with 10 % HI-FBS at 37 °C in 5 % CO₂.

Data analysis: Statistical analysis IC50 values were calculated in Graphpad Prism by non-linear regression (curve fit), dose-response inhibition, log(inhibitor) vs normalised response, variable slope

Crystallography

Crystallographic data of compounds **6**, **22**, **25**, **26**, **28** were collected at the MX1 beamline and compound **31** was collected on the MX2 beamline at the Australian Synchrotron, Melbourne, Victoria, Australia, operating at 17.4 keV ($\lambda = 0.71080 \text{ \AA}$) using an open flow of N₂ cryostream and cooled to 173(2) K for MX1 and 100(2) K for MX2. The software used for data collection and reduction of the data were Bluice²⁶ and XDS.²⁷ Crystallographic data for compounds **3**, **8**, **9**, **19** was collected on an OXFORD Gemini Ultra equipped with an OXFORD Cryosystems 700 Cryostream and cooled to 123(2) K. Data was collected with monochromatic (graphite) MoK α radiation ($\lambda = 0.71070 \text{ \AA}$) and processed using the CrysAlisProv 1.171.34.36 software;²⁸ Lorentz, polarization and absorption corrections (multi-scan) were applied. Crystallographic data for compound **27** was obtained on a Bruker X8 APEXII CCD diffractometer equipped with an OXFORD Cryosystems 700 Cryostream and cooled to 123(2) K. Data was collected with monochromatic (graphite) MoK α radiation ($\lambda = 0.71065 \text{ \AA}$) and processed using the Bruker Apex2 v2014.7-1 software;²⁹ Lorentz, polarization and absorption corrections (multi-scan – SADABS)³⁰ were applied. All compounds were solved and refined with SHELX-97.³¹ All non-hydrogen atoms were refined with anisotropic thermal parameters unless otherwise indicated and hydrogen atoms were placed in calculated positions using a riding model with C-H = 0.95-0.98 Å and $U_{iso}(H) = xU_{iso}(C)$, $x = 1.2$ or 1.5 unless otherwise indicated. A summary of crystallographic data for **3** (CCDC 1420787) is provided below in the experimental section while for compounds **6**, **8**, **9**, **19**, **22**, **25-28**, **31** (CCDC 1420788 - 1420797) it is provided in the Supporting Information.

General Procedure

General synthetic procedure (GP1): Stoichiometric equivalents of Bi(Tol)₃ and benzoic acid (1:2) were each dissolved in 5 mL of warm solvent and mixed. An excess of 30 % H₂O₂ was added and the mixture was stirred for 10 minutes and filtered. Crystals were subsequently obtained on allowing the filtrate to stand at room temperature overnight. Grignard reagents were synthesized under Schlenk conditions in Et₂O by the reaction of stoichiometric ratios of Mg turnings with 2-bromotoluene, 3-bromotoluene and 4-bromotoluene respectively. The resulting Grignard reagent was reacted with BiCl₃ in a 3:1 stoichiometric ratio to obtain the Bi(Tol)₃ product as a crystalline solid.

Synthesis of *tris-o*-tolylbismuth bis(2-ethoxybenzoate), **1**

Bi(*o*-Tol)₃ (0.200 g, 0.41 mmol), 2-ethoxybenzoic acid (125 mg, 0.83 mmol) and 100 μL 30 % H₂O₂ were reacted in warm diethyl ether according to GP. Yield: 39.0 % (0.130 g); mp. 126-128 °C; ¹H NMR (400 MHz, (CD₃)₂SO, 25 °C): δ = 8.34 (3H, dd, *J* = 7.9 Hz, 1.1 Hz, Tol CH), 7.58 (6H, m, Tol CH), 7.47 (3H, td, *J* = 7.4 Hz, 1.0 Hz, Tol CH), 7.25 (2H, m, CH), 7.07 (2H, dd, *J* = 7.6 Hz, 1.8 Hz, CH), 6.92 (2H, d, *J* = 7.9 Hz, CH), 6.78 (2H, td, *J* = 7.4 Hz, 0.8 Hz, CH), 3.90 (4H, q, *J* = 6.9 Hz, OCH₂CH₃), 2.60 (9H, s, Tol CH₃), 1.13 (6H, t, *J* = 7.0 Hz, OCH₂CH₃); ¹³C{¹H} (100 MHz, (CD₃)₂SO, 25 °C): δ = 170.9 (COO), 163.0 (BiC), 156.3 (COCH₂CH₃), 141.5 (CCH₃), 134.0 (CH_{ar}), 133.2 (CH_{ar}), 130.9 (CH_{ar}), 130.7 (CH_{ar}), 129.5 (CH_{ar}), 128.3 (CH_{ar}), 125.4 (CH_{ar}), 119.7 (CH_{ar}), 113.2 (CH_{ar}), 63.6 (CH₂), 22.9 (Tol CH₃), 14.4 (CH₃); MS ESI⁺ 208.9 [Bi], 391.0 [Bi(*o*-Tol)₂]⁺, 647.1 [Bi(*o*-Tol)₃L]⁺; ESI⁻ 165.1 [L]⁻, 721.2 [Bi(*o*-Tol)₂L₂]⁻; IR 2980 (w), 2931 (w), 2897 (w), 2115 (w), 1742 (w), 1719 (w), 1646 (w), 1597 (sh), 1475 (m), 1447 (sh), 1382 (sh), 1326 (s), 1297 (sh), 1269 (sh), 1232 (s), 1163 (sh), 1143 (sh), 1111 (sh), 1041 (sh), 988 (sh), 922 (sh), 794 (m), 742 (s), 709 (sh), 663 (sh); Elemental analysis [C₃₉H₃₉BiO₆·2H₂O] (848.28) Calculated C 55.19 H 5.11 Found C 55.20 H 4.69

Synthesis of *tris-o*-tolylbismuth bis(4-nitrobenzoate), **2**

Bi(*o*-Tol)₃ (0.200 g, 0.41 mmol), 4-nitrobenzoic acid (0.139 g, 0.83 mmol) and 100 μL 30 % H₂O₂ were reacted in warm diethyl ether according to GP. Yield: 44.6 % (0.149 g); mp. 146-148 °C; ¹H NMR (400 MHz, CDCl₃, 25 °C): δ = 8.44 (3H, dd, *J* = 1.1 Hz, 8.0 Hz, Tol CH), 8.11 (4H, d, *J* = 8.9 Hz, CH), 7.93 (4H, d, CH), 7.56 (3H, dd, *J* = 1.0 Hz, 7.5 Hz, Tol CH), 7.53 (3H, t, *J* = 7.0 Hz, Tol CH), 2.68 (9H, s, CH₃); ¹³C{¹H} (100 MHz, (CD₃)₂SO, 25 °C): δ = 168.6 (COO), 161.9 (BiC), 149.6 (CCH₃), 142.1 (CNO₂), 140.0 (CCOO), 134.7 (CH_{ar}), 133.7 (CH_{ar}), 131.6 (CH_{ar}), 130.7 (CH_{ar}), 129.0 (CH_{ar}), 123.2 (CH_{ar}), 23.8 (CH₃); MS ESI⁺ 208.9 [Bi], 391.1 [Bi(*o*-Tol)₂]⁺, 648.1 [Bi(*o*-Tol)₃L]⁺; 166.0 [L]⁻, 723.2 [Bi(*o*-Tol)₂L₂]⁻; IR 2929 (br), 2861 (br), 1646 (sh), 1601 (sh), 1519 (sh), 1474 (m), 1449 (m), 1405 (w), 1349 (m), 1292 (m), 1206 (sh), 1163 (sh), 1123 (sh), 1099 (sh), 999 (sh), 874 (sh), 819 (sh), 791 (sh), 742 (sh), 719 (sh), 669 (m); Elemental analysis [C₃₅H₂₉BiN₂O₈] (814.60) Calculated C 51.61 H 3.59 N 3.44 Found C 51.47 H 3.63 N 3.31

Synthesis of *tris-o*-tolylbismuth bis(2',4'-difluoro-4-hydroxybiphenyl-3-carboxylate), **3**

Bi(*o*-Tol)₃ (0.200 g, 0.41 mmol), Diflunisal (0.208 g, 0.83 mmol) and 100 μ L 30 % H₂O₂ were reacted in warm diethyl ether according to **GP**. Yield: 75.1 % (0.302 g); mp. 153-154 °C; ¹H NMR (400 MHz, (CD₃)₂SO, 25 °C): δ = 11.69 (2H, s, OH), 8.36 (3H, d, *J* = 7.9 Hz, *o*-CH_{ar}), 7.72 (5H, m, CH_{ar}), 7.66 (3H, t, *J* = 7.4 Hz, *m*-CH_{ar}), 7.57 (3H, t, *J* = 7.4 Hz, *p*-CH_{ar}), 7.53 (2H, d, *J* = 8.9 Hz, CH_{ar}), 7.46 (2H, q, *J* = 6.9 Hz, CH_{ar}), 7.31 (2H, t, *J* = 10.4 Hz, CH_{ar}), 7.16 (2H, td, *J* = 8.1 Hz, 1.8 Hz, CH_{ar}), 6.89 (2H, d, *J* = 8.6 Hz, CH_{ar}), 2.60 (9H, s, CH₃); ¹³C{¹H} (100 MHz, (CD₃)₂SO, 25 °C): δ = 172.6 (COO), 161.2 (BiC), 160.4 (CF), 159.8 (CF), 158.1 (CCOO), 141.7 (CCH₃), 134.8 (CH_{ar}), 134.3 (CH_{ar}), 134.0 (CH_{ar}), 132.0 (CH_{ar}), 131.3 ((F)CCHC(F)), 130.6 (CH_{ar}), 129.3 (CH_{ar}), 124.6 (*i*-C_{ar}), 123.8 (*i*-C_{ar}), 117.1 (CH_{ar}), 115.2 (COH), 112.1 (CH_{ar}), 104.5 (CH_{ar}), 23.0 (CH₃); MS ESI⁺ 208.9 [Bi], 391.1 [Bi(*o*-Tol)₂]⁺, 731.2 [Bi(*o*-Tol)₃L]⁺; ESI⁻ 249.0 [L]⁻; IR 3074 (br), 2951 (w), 1634 (m), 1593 (m) 1561 (sh), 1509 (w), 1481 (sh), 1435 (sh), 1381 (sh), 1352 (sh), 1292 (m), 1245 (s), 1223 (sh), 1140 (sh), 1102 (sh), 1033 (w), 967 (sh), 917 (w), 889 (sh), 851 (sh), 833 (sh), 743 (sh), 726 (sh), 703 (sh), 662 (sh); Elemental Analysis [C₄₇H₃₅BiF₄O₆] (980.77) Calculated C 57.56 H 3.60 Found C 57.67 H 3.88

Crystal Data for **3**: C₅₁H₄₅BiF₄O₇; M_r = 1054.85; triclinic; space group: P-1; *a* = 12.2901(3), *b* = 12.4486(3), *c* = 15.1716(4); α = 76.296(2); β = 76.185(2); γ = 84.494(2); *V* = 2187.95(9) Å³; *Z* = 2, Reflections collected/unique: 56966/14625 (*R*_{int} = 0.0449); *R*₁ values (*I* > 2 σ (*I*)) = 0.0265; *wR*(*F*²) values (*I* > 2 σ (*I*)) = 0.0503; *R*₁ values (all data) = 0.0355; *wR*(*F*²) values (all data) = 0.0539; GOF = 1.033; Temperature = 123(2) K.

Synthesis of *tris-m*-tolylbismuth bis(3,5-dimethylbenzoate), **5**

Bi(*m*-Tol)₃ (0.200 g, 0.41 mmol), 3,5-dimethylbenzoic acid (0.125 g, 0.83 mmol) and 100 μ L 30 % H₂O₂ were reacted in warm diethyl ether according to **GP**. Yield: 51.5 % (0.165 g); mp. 173-176 °C; ¹H NMR (400 MHz, (CD₃)₂SO, 25 °C): δ = 7.99 (3H, s, Tol *o*-CH), 7.96 (3H, d, ³*J* = 8.1 Hz, Tol *o*-CH), 7.61 (3H, t, ³*J* = 7.7 Hz, Tol *m*-CH), 7.47 (4H, s, *o*-CH), 7.36 (3H, d, ³*J* = 7.5 Hz, Tol *p*-CH), 7.13 (2H, s, *p*-CH), 2.35 (9H, s, Tol CH₃), 2.27 (12H, s, CH₃); ¹³C{¹H} (100 MHz, (CD₃)₂SO, 25 °C): δ = 171.8 (COO), 160.2 (BiC), 141.2 (CCH₃), 137.4 (CCH₃), 133.4 (*o*-CH₃), 132.4 (CCCO), 131.8 (CH_{ar}), 131.3 (CH_{ar}), 130.5 (CH_{ar}), 127.3 (CH_{ar}), 21.5 (CH₃), 20.7 (CH₃); MS ESI⁺ 208.97 [Bi], 346.18 [2Bi(*m*-Tol) + (*m*-Tol)H]²⁺, 391.03 [Bi(*m*-Tol)₂]⁺, 631.18 [Bi(*m*-Tol)₃(L)]⁺; ESI⁻ 149.10 [L]⁻; IR 3503 (w), 3377 (br), 3051 (w), 2917 (w), 2862 (w), 1574 (sh), 1553 (sh), 1472 (w), 1447 (w), 1385 (sh), 1347 (s), 1309 (m), 1259 (m), 1208 (w), 1168 (w), 1092 (w), 1040 (w), 999 (w), 980 (sh), 869 (w), 811 (sh), 771 (sh), 675 (sh); Elemental analysis [C₃₉H₃₉BiO₄·H₂O] (798.28) Calculated C 58.65 H 5.17 Found C 58.31 H 5.18

Synthesis of *tris-m*-tolylbismuth bis(3,5-dihydroxybenzoate), **6**

Bi(*m*-Tol)₃ (0.400 g, 0.83 mmol), 3,5-dihydroxybenzoic acid (0.256 g, 1.66 mmol) and 100 μ L 30 % H₂O₂ were reacted in warm diethyl ether according to **GP**. Yield: 64.6 % (0.377 g); mp. 170 °C (decomp.); ¹H NMR (400 MHz, (CD₃)₂SO, 25 °C): δ = 9.40 (4H, s, OH), 7.96 (3H, s, Tol *o*-CH), 7.91 (3H, d, ³*J* = 7.6 Hz, Tol *o*-CH), 7.61 (3H, t, ³*J* = 7.7 Hz, Tol *m*-CH), 7.37 (3H, d, ³*J* = 7.5 Hz, Tol *p*-CH), 6.72 (3H, d, ⁴*J* = 2 Hz, *o*-CH), 6.31 (2H, t, ⁴*J* =

2 Hz, *p*-CH), 2.36 (9H, s, Tol CH₃); ¹³C{¹H} (100 MHz, (CD₃)₂SO, 25 °C): δ = 171.7 (COO), 160.1 (BiC), 158.2 (COH), 141.2 (CCOO), 134.4 (CCH₃), 133.4 (CH_{ar}), 131.8 (CH_{ar}), 131.2 (CH_{ar}), 130.3 (CH_{ar}), 107.6 (CH_{ar}), 106.0 (CH_{ar}), 21.5 (CH₃); MS ESI⁺ 208.99 [Bi], 391.00 [Bi(*m*-Tol)₂]⁺, 635.10 [Bi(*m*-Tol)₃(L)]⁺, 725.13 [BiL]²⁺; ESI⁻ 153.08 [L]; IR 3511 (w), 3394 (w), 3157 (br), 2980 (w), 1569 (s), 1465 (m), 1465 (w), 1341 (sh), 1298 (s), 1282 (m), 1202 (w), 1155 (sh), 1097 (w), 1005 (sh), 979 (sh), 954 (w), 858 (sh), 811 (sh), 811 (sh), 785 (sh), 678 (sh); Elemental analysis [C₃₅H₃₁BiO₈·2H₂O·Et₂O] (898.28) Calculated C 52.12 H 5.05 Found C 52.01 H 5.04

Synthesis of *tris-m*-tolylbismuth bis(2-methoxybenzoate), **7**

Bi(*m*-Tol)₃ (0.200 g, 0.41 mmol), 2-methoxybenzoic acid (0.126 g, 0.83 mmol) and 100 μL 30 % H₂O₂ were reacted in warm diethyl ether according to **GP**. Yield: 47.6 % (0.153 g); mp. 145-146 °C; ¹H NMR (400 MHz, (CD₃)₂SO, 25 °C): δ = 8.08 (3H, s, Tol *o*-CH), 8.00 (3H, d, ³J = 8 Hz, Tol *o*-CH), 7.61 (3H, t, ³J = 7.7 Hz, Tol *m*-CH), 7.39 (7H, m, Tol *p*-CH + CH), 7.04 (2H, d, ³J = 8 Hz, CH), 6.91 (2H, t, ³J = 7.4 Hz, *p*-CH), 3.80 (6H, s, OCH₃), 2.37 (9H, s, Tol CH₃); ¹³C{¹H} (100 MHz, (CD₃)₂SO, 25 °C): δ = 172.1 (COO), 159.6 (BiC), 157.6 (COCH₃), 149.7 (CCH₃), 141.2 (CH_{ar}), 133.6 (CH_{ar}), 131.8 (CH_{ar}), 131.7 (CH_{ar}), 131.1 (CH_{ar}), 130.4 (CH_{ar}), 130.1 (CH_{ar}), 123.9 (CCOO), 120.0 (CH_{ar}), 112.5 (CH_{ar}), 55.8 (OCH₃), 21.5 (CH₃); MS ESI⁺ 208.99 [Bi], 391.00 [Bi(*m*-Tol)₂]⁺, 633.14 [Bi(*m*-Tol)₃(L)]⁺; ESI⁻ 151.10 [L], 693.00 [Bi(*m*-Tol)₂L₂]; IR 3045 (w), 3001 (w), 2915 (w), 2835 (w), 1601 (sh), 1581 (sh), 1542 (sh), 1457 (m), 1435 (sh), 1352 (s), 1300 (w), 1268 (sh), 1249 (m), 1177 (sh), 1162 (sh), 1142 (sh), 1097 (w), 1021 (w), 981 (sh), 857 (sh), 809 (sh), 774 (sh), 750 (sh), 704 (sh), 659 (sh); Elemental analysis [C₃₇H₃₅BiO₆] (784.66) Calculated C 56.64 H 4.50 Found C 56.22 H 4.53

Synthesis of *tris-m*-tolylbismuth bis(2-ethoxybenzoate), **8**

Bi(*m*-Tol)₃ (0.200 g, 0.41 mmol), 2-ethoxybenzoic acid (0.125 μL, 0.83 mmol) and 100 μL 30 % H₂O₂ were reacted in warm diethyl ether according to **GP**. Yield: 46.2 % (0.154 g); mp. 144-145 °C; ¹H NMR (400 MHz, (CD₃)₂SO, 25 °C): δ = 8.05 (3H, s, Tol *o*-CH), 8.01 (3H, d, ³J = 7.7 Hz, Tol *o*-CH), 7.60 (3H, t, ³J = 7.8 Hz, Tol *m*-CH), 7.36 (7H, m, Tol *p*-CH + CH), 7.02 (2H, d, ³J = 8.3 Hz, CH), 6.90 (2H, t, ³J = 7.4 Hz, *p*-CH), 4.02 (4H, q, ³J = 6.9 Hz, OCH₂CH₃), 2.35 (9H, s, Tol CH₃), 1.28 (6H, t, OCH₂CH₃); ¹³C{¹H} (100 MHz, (CD₃)₂SO, 25 °C): δ = 172.4 (COO), 160.0 (BiC), 156.9 (*i*-C_{ar}), 141.0 (CCH₃), 133.5 (CH_{ar}), 131.7 (CH_{ar}), 131.6 (CH_{ar}), 131.0 (CH_{ar}), 130.4 (CH_{ar}), 130.1 (CH_{ar}), 124.2 (CCOO), 120.0 (CH_{ar}), 113.6 (CH_{ar}), 63.9 (OCH₂CH₃), 21.4 (CH₃), 14.7 (OCH₂CH₃); MS ESI⁺ 391.2 [Bi(*m*-Tol)₂]⁺, 647.3 [Bi(*m*-Tol)₃(L)]⁺, 835.4 [Bi(*m*-Tol)₃(L)₂ + Na]⁺; ESI⁻ 165.0 [L], 721.2 [Bi(*m*-Tol)₂L₂]; IR 3052 (w), 2979 (w), 2921 (w), 1583 (sh), 1554 (sh), 1532 (w), 1472 (w), 1450 (sh), 1356 (s), 1292 (w), 1269 (sh), 1238 (s), 1164 (sh), 1146 (sh), 1113 (sh), 1035 (sh), 980 (sh), 925 (sh), 853 (sh), 811 (sh), 795 (sh), 754 (sh), 704 (m), 667 (sh); Elemental analysis [C₃₉H₃₉BiO₆] (812.72) Calculated C 57.64 H 4.84 Found C 57.11 H 4.92

Synthesis of *tris-m*-tolyl-bismuth bis(4-nitrobenzoate), **9**

Bi(*m*-Tol)₃ (0.200 g, 0.41 mmol), 4-nitrobenzoic acid (0.138 g, 0.83 mmol) and 100 μ L 30 % H₂O₂ were reacted in warm diethyl ether according to **GP**. Yield: 41.9 % (0.140 g); mp. 170-172 °C; ¹H NMR (400 MHz, (CD₃)₂SO, 25 °C): δ = 8.15 (8H, br. dd, ³J = 8.6 Hz, ⁴J = 3.0 Hz, *o*-CH, *m*-CH), 8.02 (3H, s, Tol *o*-CH), 7.98 (3H, d, ³J = 8.0 Hz, Tol *o*-CH), 7.65 (3H, t, ³J = 7.7 Hz, Tol *m*-CH), 7.40 (3H, d, ³J = 7.5 Hz, Tol *p*-CH), 2.37 (9H, s, Tol CH₃); ¹³C{¹H} (100 MHz, (CD₃)₂SO, 25 °C): δ = 158.3 (BiC), 149.5 (CNO₂), 147.6 (CCH₃), 141.7 (CCOO), 133.6 (CH_{ar}), 132.2 (CH_{ar}), 131.6 (CH_{ar}), 130.7 (CH_{ar}), 130.6 (CH_{ar}), 123.5 (CH_{ar}), 21.5 (CH₃); MS ESI⁺ 209.0 [Bi], 391.1 [Bi(*m*-Tol)₂]⁺, 648.3 [Bi(*m*-Tol)₃(L)]⁺; ESI⁻ 166.0 [L]⁻, 723.1 [Bi(*m*-Tol)₂L₂]⁻; IR 2920 (w), 1622 (m), 1583 (sh), 1523 (sh), 1467 (w), 1406 (sh), 1331 (s), 1162 (w), 1130 (sh), 1099 (sh), 1011 (sh), 981 (sh), 876 (sh), 831 (sh), 777 (sh), 720 (sh), 676 (sh); Elemental analysis [C₃₅H₂₉BiN₂O₈] (814.60) Calculated C 51.61 H 3.59 N 3.44 Found C 51.18 H 3.31 N 3.29

Synthesis of *tris-m*-tolylbismuth bis(2-[[3-trifluoromethyl]phenyl]amino)benzoate), **10**

Bi(*m*-Tol)₃ (0.200 g, 0.41 mmol), flufenamic acid (0.233 g, 0.83 mmol) and 100 μ L 30 % H₂O₂ were reacted in warm diethyl ether according to **GP**. Yield: 66.4 % (0.284 g); mp. 143-147 °C; ¹H NMR (400 MHz, (CD₃)₂SO, 25 °C): δ = 9.57 (2H, s, NH), 8.03 (3H, s, *o*-CH_{ar}), 7.97 (3H, d, J = 7.9 Hz, *o*-CH_{ar}), 7.88 (2H, d, J = 7.5 Hz, CH_{ar}), 7.59 (3H, t, J = 7.7 Hz, CH_{ar}), 7.49 (2H, t, J = 7.7 Hz, CH_{ar}), 7.35 (10H, m, CH_{ar}), 7.26 (5H, m, CH_{ar}), 6.85 (2H, t, CH_{ar}), 2.26 (9H, s, CH₃); ¹³C{¹H} (100 MHz, (CD₃)₂SO, 25 °C): δ = 159.4 (BiC), 142.4 (C(NH)), 141.6 (C(NH)), 133.6 (CH_{ar}), 132.5 (CH_{ar}), 132.0 (CH_{ar}), 131.4 (CH_{ar}), 130.5 (CH_{ar}), 130.4 (CH_{ar}), 130.3 (CH_{ar}), 130.1 (CH_{ar}), 124.9 (*i*-C_{ar}), 123.1 (*i*-C_{ar}), 122.5 (CH_{ar}), 119.2 (CH_{ar}), 117.9 (CH_{ar}), 115.2 (CH_{ar}), 21.2 (CH₃); MS ESI⁺ 209.0 [Bi], 391.2 [Bi(*m*-Tol)₂]⁺, 762.3 [Bi(*m*-Tol)₃L]⁺; ESI⁻ 236.0 [L-COO]⁻, 280.0 [L]⁻; IR 3256 (br), 3058 (w), 2922 (w), 1583 (sh), 1561 (m), 1513 (m), 1462 (sh), 1462 (w), 1352 (sh), 1333 (sh), 1272 (s), 1214 (m), 1160 (sh), 1116 (sh), 1067 (sh), 998 (sh), 979 (sh), 931 (sh), 902 (w), 860 (sh), 796 (sh), 748 (sh), 696 (sh), 665 (sh); Elemental analysis [C₄₉H₃₉BiF₆N₂O₄·2H₂O] (1078.28) Calculated C 54.55 H 4.02 N 2.60 Found C 54.72 H 3.65 N 2.71

Synthesis of *tris-m*-tolylbismuth bis(2-(acetoxyl)benzoate), **11**

Bi(*m*-Tol)₃ (0.200 g, 0.41 mmol), Aspirin (0.150 g, 0.83 mmol) and 100 μ L 30 % H₂O₂ were reacted in warm diethyl ether according to **GP**. Yield: 76.9 % (0.265 g); mp. 129-132 °C; ¹H NMR (400 MHz, (CD₃)₂SO, 25 °C): δ = 7.92 (3H, s, Tol *o*-CH), 7.88 (3H, d, ³J = 7.8 Hz, Tol *o*-CH), 7.75 (2H, d, ³J = 7.6 Hz, *o*-CH), 7.63 (3H, t, ³J = 7.6 Hz, Tol *m*-CH), 7.52 (2H, t, ³J = 7.7 Hz, *p*-CH), 7.41 (3H, d, ³J = 7.6 Hz, Tol *p*-CH), 7.29 (2H, t, ³J = 7.3 Hz, asp *m*-CH), 7.08 (2H, d, ³J = 7.9 Hz, *m*-CH), 2.38 (9H, s, Tol CH₃), 2.00 (6H, s, asp CH₃); ¹³C{¹H} (150 MHz, (CD₃)₂SO, 25 °C): δ = 170.3 (COO), 169.1 (BiC), 159.3 (*i*-C_{ar}), 149.7 (*i*-C_{ar}), 141.6 (CCH₃), 133.4 (CH_{ar}), 132.7 (CH_{ar}), 131.9 (CH_{ar}), 131.4 (CH_{ar}), 131.3 (CH_{ar}), 130.3 (CH_{ar}), 126.6 (*i*-C_{ar}), 125.9 (CH_{ar}), 123.5 (CH_{ar}), 21.5 (CH₃), 20.7 (CH₃); MS ESI⁺ 209.0 [Bi], 391.2 [Bi(*m*-Tol)₂]⁺, 661.3 [Bi(*m*-Tol)₃L]⁺, 863.2 [Bi(*m*-Tol)₃L₂ + Na]⁺; IR 2920 (w), 1755 (sh), 1624 (sh), 1592 (sh), 1553 (m), 1473 (m), 1448 (m), 1355 (sh), 1324 (sh), 1220 (sh), 1192 (sh),

1089 (sh), 1040 (w), 1012 (w), 980 (m), 954 (w), 919 (m), 878 (w), 850 (w), 809 (sh), 768 (sh), 748 (sh), 703 (sh), 672 (sh); Elemental Analysis [C₃₉H₃₅BiO₈·2H₂O] (876.23) Calculated C 53.43 H 4.48 Found C 53.00 H 4.04

References

1. L. Kedzierski, A. Sakthianandeswaren, J. M. Curtis, P. C. Andrews, P. C. Junk and K. Kedzierska *Curr. Med. Chem.*, 2009, **16**, 599-614.
2. WHO, Leishmaniasis, <http://www.who.int/leishmaniasis/en/>, Accessed August 2015.
3. W. L. Roberts and P. M. Rainey, *Antimicrob. Agents Chemother.*, 1993, **37**, 1842-1846.
4. W. L. Roberts, W. J. McMurray and P. M. Rainey, *Antimicrob. Agents Chemother.*, 1998, **42**, 1076-1082.
5. F. Frezard, C. Demicheli and R. R. Ribeiro, *Molecules*, 2009, **14**, 2317-2336.
6. Ashutosh, S. Sundar and N. Goyal, *Med. Microbiol.*, 2007, **56**, 143-153.
7. S. Sundar, *Trop. Med. Int. Health*, 2001, **6**, 849-854.
8. S. Sundar and J. Chakravarty, *J. Global Infect. Dis.*, 2010, **2**, 159-166.
9. S. Sundar and P. L. Olliaro, *Ther. Clin. Risk Manag.*, 2007, **3**, 733-740.
10. S. Yan, F. Li, K. Ding and H. Sun, *J. Biol. Inorg. Chem.*, 2003, **8**, 689-697.
11. X. Wang and H. Sun, in *Comprehensive Inorganic Chemistry II (Second Edition)*, ed. J. R. Poeppelemeier, Elsevier, Amsterdam, 2013, pp. 975-986.
12. S. Wyllie, M. L. Cunningham and A. H. Fairlamb, *J. Biol. Chem.*, 2004, **279**, 39925-39932.
13. M. I. Ali, M. K. Rauf, A. Badshah, I. Kumar, C. M. Forsyth, P. C. Junk, L. Kedzierski and P. C. Andrews, *Dalton Trans.*, 2013, **42**, 16733-16741.
14. H. L. Seng and E. R. T. Tiekink, in *Comprehensive Inorganic Chemistry II (Second Edition)*, ed. J. R. Poeppelemeier, Amsterdam, 2013, pp. 951-974.
15. P. C. Andrews, R. Frank, P. C. Junk, L. Kedzierski, I. Kumar and J. G. MacLellan, *J. Inorg. Biochem.*, 2011, **105**, 454-461.
16. P. C. Andrews, P. C. Junk, L. Kedzierski and R. M. Peiris, *Aus. J. Chem.*, 2013, **66**, 1297-1305.
17. P. C. Andrews, V. L. Blair, R. L. Ferrero, P. C. Junk, L. Kedzierski and R. M. Peiris, *Dalton Trans.*, 2014, **43**, 1279-1291.
18. Y. C. Ong, V. L. Blair, L. Kedzierski and P. C. Andrews, *Dalton Trans.*, 2014, **43**, 12904-12916.
19. V. V. Sharutin, O. K. Sharutina and V. S. Senchurin, *Russ. J. Inorg. Chem.*, 2013, **58**, 1470-1474.
20. G. B. Deacon and R. J. Phillips, *Coord. Chem. Rev.*, 1980, **33**, 227-250.
21. M. Vermeersch, R. I. da Luz, K. Toté, J.-P. Timmermans, P. Cos and L. Maes, *Antimicrob. Agents Chemother.*, 2009, **53**, 3855-3859.
22. D. H. R. Barton, N.Y. Bhatnagar, J.-P. Finet, W. B. Motherwell, *Tetrahedron*, 1986, **42**, 3111-3122.
23. J. Mikus and D. Steverding, *Parasitol. Int.*, 2000, **48**, 265-269.
24. K. Lackovic, J. P. Parisot, N. Sleebs, J. B. Baell, L. Debien, K. G. Watson, J. M. Curtis, E. Handman, I. P. Street and L. Kedzierski, *Antimicrob. Agents Chemother.*, 2010, **54**, 1712-1719.
25. E. Handman, R. E. Hocking, G. F. Mitchell and T. W. Spithill, *Mol. Biochem. Parasitol.*, 1983, **7**, 111-126.

26. T. M. McPhillips, S. E. McPhillips, H.-J. Chiu, A. E. Cohen, A. M. Deacon, P. J. Ellis, E. Garman, A. Gonzalez, N. K. Sauter, R. P. Phizackerley, S. M. Soltis and P. Kuhn, *J. Synchro. Rad.*, 2002, **9**, 401-406.
27. W. Kabsch, *J. Appl. Crystallogr.*, 1993, **26**, 795-800.
28. *CrysAlisPro v1.171.34.36*, 2010, Oxford Diffraction Ltd (Agilent Technologies), Oxfordshire, UK.
29. *Bruker Apex2 v2014.7-1*, 2014, Bruker AXS, Madison, US.
30. G. M. Sheldrick, *SADABS v2.30*, 2002, University of Gottingen.
31. G. M. Sheldrick, *Acta Crystallogr. Sect. A*, 2008, **64**, 112-122.

A fluorescent, photochromic and thermochromic trifunctional material based on a layered metal-viologen complex

Fang Wan, Li-Xia Qiu, Liang-Liang Zhou, Yan-Qiong Sun* and Yi You

College of Chemistry, Fuzhou University, Fuzhou, Fujian 350108, People's Republic of China.

E-mail: sunyq@fzu.edu.cn

A 2D layered viologen-based Zinc complex exhibits the rare discolored function of reversible photochromism and thermochromism. Interestingly, the fluorescence of it can be switched by visible light irradiation and heating in air.

